MOLECULAR AND CELLULAR BIOLOGY, Apr. 2002, p. 2821–2829 Vol. 22, No. 8
0270-7306/02/$04.00+0 DOI: 10.1128/MCB.22.8.2821–2829.2002

Impaired Cardiac Contractility Response to Hemodynamic Stress in S100A1-Deficient Mice

Xiao-Jun Du,[1] Timothy J. Cole,[1] Nora Tenis,[2] Xiao-Ming Gao,[1] Frank Köntgen,[3]† Bruce E. Kemp,[2,4] and Jörg Heierhorst[2,4]*

Baker Medical Research Institute, Melbourne, Victoria 8008,[1] The Walter-and-Eliza-Hall Institute, Parkville, Victoria 3050,[3] and St. Vincent's Institute of Medical Research[2] and Department of Medicine, St. Vincent's Hospital, The University of Melbourne,[4] Fitzroy, Victoria 3065, Australia

Received 24 October 2001/Returned for modification 10 December 2001/Accepted 22 January 2002

Ca^{2+} signaling plays a central role in cardiac contractility and adaptation to increased hemodynamic demand. We have generated mice with a targeted deletion of the S100A1 gene coding for the major cardiac isoform of the large multigenic S100 family of EF hand Ca^{2+}-binding proteins. S100A1$^{-/-}$ mice have normal cardiac function under baseline conditions but have significantly reduced contraction rate and relaxation rate responses to β-adrenergic stimulation that are associated with a reduced Ca^{2+} sensitivity. In S100A1$^{-/-}$ mice, basal left-ventricular contractility deteriorated following 3-week pressure overload by thoracic aorta constriction despite a normal adaptive hypertrophy. Surprisingly, heterozygotes also had an impaired response to acute β-adrenergic stimulation but maintained normal contractility in response to chronic pressure overload that coincided with S100A1 upregulation to wild-type levels. In contrast to other genetic models with impaired cardiac contractility, loss of S100A1 did not lead to cardiac hypertrophy or dilation in aged mice. The data demonstrate that high S100A1 protein levels are essential for the cardiac reserve and adaptation to acute and chronic hemodynamic stress in vivo.

Transient elevations of intracellular Ca^{2+} levels are a major signaling mechanism in the regulation of eukaryotic cell functions (5). These effects are mediated by Ca^{2+} sensor proteins that contain specific Ca^{2+}-binding motifs such as EF hands (e.g., calmodulin) or C2 domains (e.g., protein kinase C). The largest subfamily of EF hand Ca^{2+}-binding proteins is comprised of the S100 proteins, with 20 different genes identified in the human genome (8, 40). S100 proteins are typically homodimers of ~10 kDa subunits, but heterodimerization adds considerably to the complexity of this multiprotein family. The majority of S100 genes are clustered on a 1.6-Mbp segment of human chromosome 1 (1q21). This gene cluster as such is conserved on murine chromosome 3, although the mouse S100 genes are arranged in a different linear order than in the human genome (37). The S100 genes are expressed in a highly tissue-specific and cell-type-specific manner. While S100A1 and S100B are widely distributed, with highest levels in cardiomyocytes and glial cells, respectively, others are more restricted to certain cell types or tissues (8).

Most S100 proteins are thought to act intracellularly by regulating effector proteins in a Ca^{2+}-dependent manner analogous to calmodulin (8, 17). However, some S100 proteins have extracellular functions as cytokines and chemokines by activating the receptor for advanced glycosylation end products (20). Numerous intracellular target proteins and functions have been proposed for S100 proteins based on studies in vitro. For example, S100A1 was found to inhibit the phosphorylation of cytoskeletal proteins (glial fibrillary acidic protein and tau) and transcription factors (MyoD) by blocking phosphorylation sites, to regulate assembly of microtubuli, actin filaments, and intermediate filaments, and to regulate the activity of metabolic enzymes (glycogen phosphorylase, phosphoglucomutase, and aldolase), signaling enzymes (adenylate and guanylate cyclases), and basic helix-loop-helix transcription factors (2, 8, 40, 47). In addition, S100A1 can stimulate Ca^{2+}-induced Ca^{2+} release from isolated sarcoplasmic reticulum (SR) vesicles (14), directly increase the open probability (i.e., activation) of reconstituted skeletal muscle ryanodine receptors (44), and stimulate the catalytic activity of the invertebrate giant protein kinase twitchin more than 1,000-fold (17).

Despite extensive in vitro studies since the initial identification of S100 proteins almost 40 years ago (8), their physiological functions have remained largely elusive. Gene-targeted mouse models have been reported in two cases: S100A8$^{-/-}$ is lethal, and the phenotype indicates a role for the protein in preventing maternal rejection of the implanted embryo (34); S100B$^{-/-}$ mice have no gross abnormal phenotype, but cultured astrocytes show signs of altered Ca^{2+} metabolism indicative of a buffering function (46).

The S100A1 protein is most abundant in cardiomyocytes (22, 25) and several S100 proteins have been circumstantially linked to roles in heart disease (8). S100A1 is reduced in end-stage heart failure (36), a clinical marker of ischemia (24), and a possible target of cardioprotective drugs (32). S100B is normally not expressed in the heart but is induced after myocardial infarction in humans, and transgenic S100B overexpression has a cardioprotective effect in mice (45). Two other cardiac S100 proteins, S100A4 and S100A11, are also upregulated following chronic β-adrenergic stimulation of rat hearts (21), but functional consequences are unknown.

* Corresponding author. Mailing address: St. Vincent's Institute of Medical Research, 9 Princes St., Fitzroy, Victoria 3065, Australia. Phone: 61-3-9288-2503/2515. Fax: 61-3-9416-2676. E-mail: heier@ariel.its.unimelb.edu.au.

† Present address: Ozgene Pty. Ltd., Nedlands 6909, Western Australia, Australia.

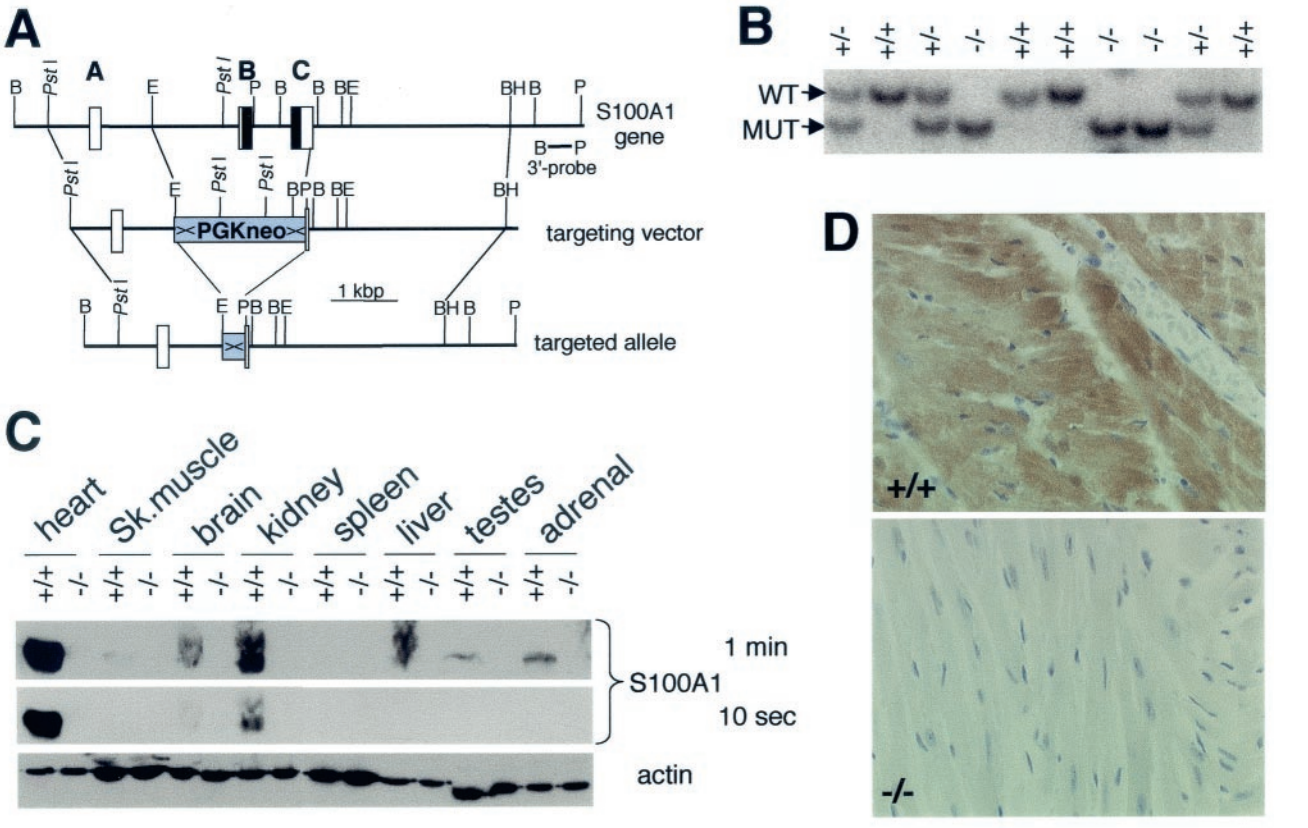

FIG. 1. Generation and analysis of S100A1-targeted mice. (A) Map of the murine S100A1 gene, targeting vector, and targeted allele after Cre/LoxP recombination. Boxes and bold letters indicate exons, with protein-coding sequences shown in black. Selected restriction enzyme cleavage sites are indicated: B, *Bgl*II; BH, *Bam*HI; E, *Eco*RI; P, *Pvu*II. ×, *loxP*. (B) Southern blot genotyping of a litter of an S100A1 heterozygous cross. WT, wild-type allele; MUT, mutant allele. (C) Immunoblot analysis of tissue extracts from S100A1$^{-/-}$ mice and wild-type littermates. Two S100A1 exposures and an actin loading control are shown. (D) Immunohistochemistry of wild-type and mutant left ventricles. The localization of S100A1 is indicated by the brown color.

In order to gain insight into the physiological function of S100A1, we have generated a mouse strain with a targeted deletion of the S100A1 protein-coding sequence. Here we show that S100A1 null mice have dramatically reduced responses to acute and chronic hemodynamic stress that are at least in part caused by reduced cardiac Ca^{2+} sensitivity. Normal contractility under baseline conditions and the absence of spontaneous cardiomyopathy in S100A1 null mice indicate that the protein has a specific function in the cardiac reserve required for adaptation to increased hemodynamic demand. Moreover, we found a haploinsufficient phenotype for the response to acute β-adrenergic stimulation in S100A1 heterozygotes, indicating a surprisingly low degree of functional redundancy in this large multigene family.

MATERIALS AND METHODS

Generation of S100A1 gene-targeted mice. The S100A1 gene was isolated from a mouse 129Sv genomic DNA library (3) in the λ-DASH II cloning vector by hybridization of plaque lifts using a radiolabeled rat S100A1 cDNA probe (18). Restriction fragments were subcloned into pBluescript vectors for mapping and sequence analysis. The sequence of a continuous 5,065-bp segment encompassing a 975-bp upstream regulatory sequence, three exons (with the protein coding sequence contained in exons B and C), two introns, and an 800-bp downstream sequence was determined.

The S100A1 targeting vector contained a 5′ 1.6-kbp *Pst*I-*Eco*RI fragment, followed by the PGK-neo marker flanked by *loxP* sites, an engineered diagnostic *Pvu*II site, and a 3′ 3.1-kbp *Apa*LI-*Bam*HI fragment (Fig. 1A). Electroporated W9.5 ES cell clones (3) containing a single targeted allele were identified by Southern blot analysis using a 3′ 700-bp *Bgl*II-*Pvu*II probe located outside the targeting vector (Fig. 1A), and correct 5′ insertion was confirmed by PCR. S100A1-targeted ES cells were microinjected into C57BL/6 blastocysts, and chimera were crossed with a strain expressing Cre in the germ line (41) to delete the PGK-neo cassette. S100A1$^{+/-}$ mice lacking the PGK-neo marker in the targeted allele were selected for heterozygous crosses and have a mixed 129Sv-C57BL/6 genetic background. Offspring were genotyped by Southern blotting of *Pvu*II-digested tail DNA with the *Bgl*II-*Pvu*II probe indicated in Fig. 1A. Experiments were approved by Baker Institute and St. Vincent's Hospital animal ethics committees.

Mouse cardiology. For cardiac catheterizations (9), mice were anesthetized by intraperitoneal (i.p.) injection with a mixture of pentobarbitone (8 mg/100 g of body weight) and atropine (0.12 mg/100 g) and placed on a heating pad. A 1.4-F Millar catheter (Millar Instrument Co.), with the frequency response flat to 10 kHz, was inserted into the right main carotid artery and advanced into the left ventricle. Left-ventricular pressure and maximal rates of its increase and decay (dP/dt_{max} and dP/dt_{min}) were recorded, and heart rates were derived from pulse signals.

For thoracic aorta constrictions (TAC), mice were anesthetized by i.p. injection with a mixture of ketamine (8 mg/100 g), xylazine (2 mg/100 g), atropine (0.06 mg/100 g), and the pain reliever carprofen (Zenecarp; 0.1 mg/100 g). Animals were intubated via the larynx and ventilated (tide volume, 0.5 ml at 100 strokes/min). After midline incisions at the sternum, aortas were dissected between the right innominate and the left carotid arteries and constricted by 60 to 70% to a lumen size of 0.4 mm (9, 38). Sham-operated mice were subjected to similar surgery except for the constriction of the aorta. Three weeks after TAC,

the increment of systolic arterial pressures proximal to the constriction site was similar among the three genotypes (data not shown), implying an equal degree of pressure overload.

For perfusion experiments (11), mice were anesthetized with pentobarbitone (8 mg/100 g, i.p.) and heparinized (20 U/100 g, i.p.). Ascending aortas were cannulated with a metal cannula made from a 23-gauge needle, and heart perfusions in situ were started within 2 to 3 min of opening the chest with Krebs-Henseleit solution (145 mM Na^+, 4 mM K^+, 1.05 mM Mg^{2+}, 155 mM Cl^-, 25 mM HCO_3^-, 0.5 mM PO_4^{3-}, 11 mM glucose, 27 μM EDTA; gassed with 95% O_2–5% CO_2, pH 7.4, 37°C) at a constant coronary flow rate (3 ml/min) delivered by a peristaltic pump. Ca^{2+} was infused into the perfusate through a three-way connector. Pulmonary vessels were tied, resulting in an isolated but filled left ventricle allowing the use of a 1.4-F Millar microtip pressure transducer catheter for measurement of the ventricular pressure and its first derivatives (dP/dt) by placing the catheter in the left-ventricular cavity via the apex.

Transthoracic echocardiography was performed with a Hewlett-Packard Sonos 5500 ultrasound machine with a 15 MHz linear transducer as described previously (10). Mice were anesthetized (6 mg of ketamine/100 g, 1.2 mg of xylazine/100 g, 0.06 mg of atropine/100 g) and placed on a heating pad. After a short-axis two-dimensional image of the left ventricle was obtained at a level close to the papillary muscles, a two-dimensional guided M-mode trace crossing the anterior and posterior wall was recorded at a sweep speed of 100 mm/s. Measurements of M-mode tracings using the leading-edge technique were averaged from 2 cardiac cycles. Following determination of baseline parameters, mice were injected i.p. with 0.5 μg of isoproterenol/100 g as a bolus, and echo images were acquired 5 min after the injection. In separate experiments, baseline parameters were also determined in unanesthetized conscious mice.

After the completion of the functional measurements, mice were euthanized by pentobarbitone overdose. Hearts were immersed in saline on ice, and ventricles and atria were dissected and weighed. Unless stated otherwise, all experiments were performed on 5-month-old animals.

Results are expressed as means ± standard errors. For parametric data, between-group comparisons were made by using analysis of variance followed by an unpaired Student *t* test. A P value of <0.05 was considered significant.

Immunoblots and RNA blots. Tissue samples were ground to a fine powder under liquid N_2 using a mortar and pestle and lysed in protein buffer (20 mM HEPES [pH 7.4], 1 mM EGTA, 5 mM magnesium acetate, 1 mM dithiothreitol, protease inhibitor cocktail [Sigma], 1% Triton X-100, 5 mM sodium pyrophosphate, 50 sodium fluoride) or RNeasy buffer (Qiagen). Protein extracts were separated by sodium dodecyl sulfate (SDS)-polyacrylamide gel electrophoresis, transferred onto polyvinylidene difluoride membranes, and probed with antibodies against actin (Chemicon), calmodulin (Upstate Biotechnology), desmin (Santa Cruz Biotechnology), phospholamban (PLB) and phosho-Ser^{16}-PLB (Research Diagnostics), S100A1 (19), sarcoendoplasmic reticulum Ca^{2+} ATPase 2a (SERCA-2a; Santa Cruz Biotechnology), or vimentin (Santa Cruz Biotechnology), followed by secondary peroxidase-conjugated antibodies and enhanced chemiluminescence reagents (Amersham Pharmacia). Left-ventricular total RNA was isolated with RNeasy kits (Qiagen), and 0.5 μg per sample was transferred onto GeneScreen Plus membranes (NEN) with a slot blot apparatus (Bio-Rad), hybridized with ^{32}P-labeled probes using standard conditions, and analyzed by using phosphorimaging and Molecular Dynamics software.

Histology, immunohistochemistry, and electron microscopy. Hearts were fixed in 10% formalin in phosphate-buffered saline and embedded in paraffin for serial sections. Sections (5 μm) were stained with hematoxylin-eosin or 0.1% picrosirius red for determining collagen content and myocyte cross-sectional area. Picrosirius red-stained sections collected at the ventricular equator were used for measuring myocyte transverse cross-sectional areas. Seven or eight fields were randomly chosen, 8 to 10 cells per field were measured, and the average for 60 to 70 cells was used.

For immunohistochemistry, paraformaldehyde-fixed tissue sections were probed with the S100A1 antibody and peroxidase-conjugated anti-rabbit antibodies, developed with diaminobenzidine, and counterstained with hematoxylin.

Protein kinase and receptor density assays. Mouse hearts were perfused in situ for 13 min to wash out endogenous β-agonists, with inclusion of 1 μM isoproterenol during the last 3 min in the stimulated group. Hearts were snap-frozen in liquid N_2, and left-ventricular protein extracts were prepared in 10 volumes of protein buffer. Extracts were diluted twofold in kinase buffer (20 mM Tris [pH 7.4], 10 mM magnesium acetate, 0.1 mM dithiothreitol, 0.05% Tween 20, 0.4 mM ATP, 0.25 μCi [γ-^{32}P]ATP [specific activity, 3,000 Ci/mmol; Amersham]/μl), reactions were started by addition of 10 μM cyclic AMP (cAMP), mixtures were incubated at 30°C for 5 min, and reactions were terminated by the addition of 25 mM EDTA. Samples were boiled in SDS sample buffer and separated in 5 to 18% polyacrylamide gradient gels. Gels were stained with Coomassie brilliant blue, destained, dried under vacuum, and analyzed by phosphorimaging (Molecular Dynamics).

Left-ventricular β-adrenoceptor densities were measured by incubating myocardial membrane proteins with 100 pM [^{125}I](−)-iodocyanopindalol (2,200 Ci/mmol; NEN) for 1 h in the presence of 10^{-10} to 10^{-4} M L-isoproterenol (Sigma), followed by rapid filtration through Whatman GF/C filters and gamma counting of dried filters. The data were analyzed with the Allfit program.

Nucleotide sequence accession number. The sequence of the continuous 5,065-bp segment determined here has been deposited in GenBank with accession number AF368423.

RESULTS

Generation of S100A1 gene-targeted mice. The S100A1 gene was isolated from a mouse 129Sv genomic DNA library and contains three exons with the entire protein coding sequence contained in exons B and C (Fig. 1A). A targeting vector was designed to delete the entire S100A1 protein-coding sequence from the targeted allele by homologous recombination (Fig. 1A). Chimeric animals generated from $S100A1^{+/-}$ embryonic stem cell clones were bred with transgenic mice expressing the Cre recombinase in germ line cells (41) for deletion of the *loxP*-flanked selectable neomycin marker in order to avoid potential epigenetic effects resulting from the PGK-neomycin cassette (33) (Fig. 1A). Heterozygote crosses resulted in offspring with all three genotypes (Fig. 1B) in approximately Mendelian proportions (73 $S100A1^{+/+}$, 125 $S100A1^{+/-}$, 79 $S100A1^{-/-}$), indicating that the S100A1 protein is not essential for embryonic development. $S100A1^{-/-}$ mice and heterozygotes had no overt gross phenotypic alterations, and no increased morbidity and mortality was observed in animals up to 16 months of age.

Immunoblot analysis using an S100A1-specific antibody demonstrated the absence of S100A1 protein in $S100A1^{-/-}$ mice in all tissues where it is normally expressed in wild-type animals (Fig. 1C). A shorter exposure of the same blot confirmed that it is expressed at the highest levels in the heart (Fig. 1C). Immunohistochemical analyses showed that S100A1 is highly expressed in wild-type cardiomyocytes and is not apparent in other cell types of the same sections and, again, demonstrated the absence of the protein in $S100A1^{-/-}$ mice (Fig. 1D). S100A1 staining intensity was highest in the left ventricle and decreased according to compartmental workloads, with progressively lower levels in the order of left atrium, right ventricle, and right atrium (data not shown). Using quantitative immunoblots of heart extracts from 2-month-old animals, we estimate that the total S100A1 concentration in wild-type hearts is ~5 μM (data not shown). Corrected for nonmuscular tissue and lower expression in other compartments, this indicates that the normal S100A1 concentration in left-ventricular cardiomyocytes is in excess of 10 μM. S100A1 levels in heterozygotes under basal conditions were approximately half of the wild-type levels in 2-, 5-, and 16-month-old animals (data not shown). Based on RNA blots, there was no compensatory upregulation of S100B, S100A4, or S100A11 levels (i.e., the other S100 isoforms previously linked to cardiac functions) in S100A1 null or heterozygous mice (data not shown).

Reduced contractile responses to acute β-adrenergic stimulation in S100A1 null and heterozygous mice. The high S100A1 levels in the heart prompted us to search for a cardiac phenotype in S100A1-deficient mice. Despite the loss of S100A1, cardiac morphology was histologically normal in

TABLE 1. Echocardiography of S100A1 null and wild-type mice ($n = 10$ per group)[a]

Group	Heart rate (beats/min)	LVEDd (mm)	LVEDs (mm)	FS (%)
Wild type				
KXA	417 ± 17	3.5 ± 0.2	2.2 ± 0.2	38 ± 3
KXA + isoproterenol	621 ± 12	2.8 ± 0.1	0.9 ± 0.1	69 ± 2
Conscious	648 ± 30	2.8 ± 0.1	1.2 ± 0.1	60 ± 3
S100A1 null				
KXA	384 ± 15	3.6 ± 0.2	2.4 ± 0.2	32 ± 2
KXA + isoproterenol	594 ± 13	2.8 ± 0.1	1.1 ± 0.1	62 ± 2[b]
Conscious	601 ± 28	3.1 ± 0.1	1.5 ± 0.1	52 ± 4

[a] LVEDd, left-ventricular end diastolic diameter; LVEDs, left-ventricular end systolic diameter; FS, fractional shortening {FS = [(LVEDd − LVEDs)/LVEDd] × 100}; KXA, ketamine-xylazine-atropine anesthetized. Data are means ± standard errors.
[b] $P < 0.05$ versus the wild-type value.

S100A1 null and heterozygous animals (Fig. 1D and data not shown). To explore if S100A1 is required for normal cardiac function in vivo, we performed an echocardiographic analysis on S100A1 null mice and wild-type littermates (Table 1). In these experiments, both anesthetized and conscious S100A1 null mice had similar heart rates but slightly reduced left-ventricular fractional shortening rates compared to wild-type mice. Interestingly, fractional shortening in anesthetized S100A1 null mice injected with the β-adrenergic agonist isoproterenol was significantly reduced compared to that in similarly treated wild-type mice, indicating that S100A1 may be particularly important in the inotropic response to β-adrenergic stimulation.

To more accurately assess this possibility, we placed microcatheters in the left ventricles of another group of 10 anesthetized animals per genotype for intravital pressure measurements. Under baseline conditions, all mice had similar heart rates (Fig. 2A), left-ventricular systolic pressures (Fig. 2B), and maximal left-ventricular contraction rates (dP/dt_{max}) (Fig. 2C) and relaxation rates (dP/dt_{min}) (Fig. 2D), indicating an essentially normal cardiac function at rest in S100A1 null and heterozygous mice. To test if S100A1 is indeed involved in the response to acute hemodynamic stress, the mice were then intravenously injected with increasing doses of the β-adrenergic agonist isoproterenol. While all mice had a normal chronotropic response to β-adrenergic stimulation with ~30% increased heart rates (Fig. 2A), the left-ventricular systolic pressure increase was almost completely abolished in $S100A1^{-/-}$ mice, in contrast to a doubling of left-ventricular systolic pressure in the wild type (Fig. 2B). Further analyses revealed that the abolished pressure response in $S100A1^{-/-}$ mice was associated with severely impaired left-ventricular maximal contraction rates (inotropic response; dP/dt_{max}) (Fig. 2D) and relaxation rates (lusitropic response; dP/dt_{min}) (Fig. 2D) in response to β-adrenergic stimulation, relative to the wild type. Surprisingly, the left-ventricular pressure and inotropic and lusitropic responses were also impaired in S100A1 heterozygotes to an extent similar to that in S100A1 null mice (Fig. 2), demonstrating that high S100A1 levels are essential for the cardiac reserve in response to acute hemodynamic stress in vivo.

Considering the normal chronotropic response to β-adrenergic stimulation as an internal control, it is extremely unlikely that the reduced contractile responses in S100A1 null and heterozygous mice merely represent different sensitivities to the anesthetics. The fact that S100A1 null mice also have significantly reduced left-ventricular fractional shortening in response to isoproterenol stimulation compared to the wild type under conditions where heart rates are similar to those of conscious animals (Table 1) indicates that the reduced contractile response is indeed physiologically relevant. Finally, the more dramatic contractile impairment of S100A1-deficient mice in the catheter experiments (which measure isovolumic and isometric contractility of the left ventricle while the valves are closed) than in the echocardiography (where fractional shortening measures muscle shortening under isotonic conditions after opening of the aortic valve) indicates that S100A1 is more critical for isometric than isotonic force production in the heart.

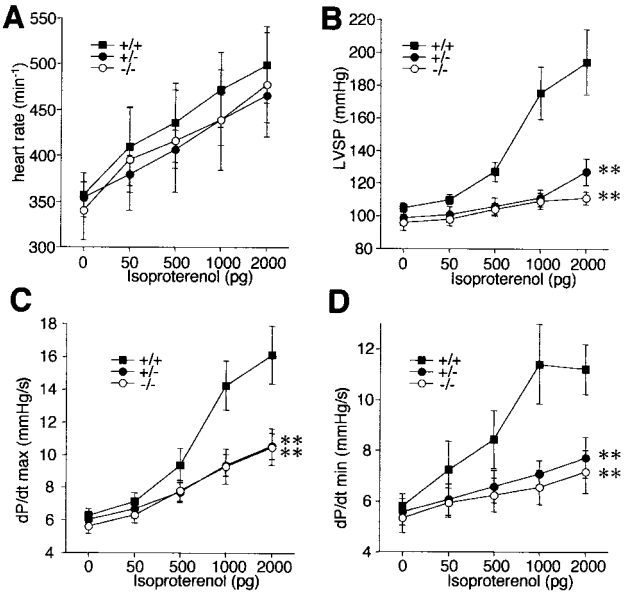

FIG. 2. β-Adrenergic cardiac response in intact animals measured with a microcatheter placed in the left ventricle. (A) Heart rates; (B) left-ventricular systolic pressure (LVSP); (C) maximal contraction rates (dP/dt_{max}, in thousands); (D) maximal relaxation rates (dP/dt_{min}, in thousands). Isoproterenol was intravenously given as a bolus as indicated. **, $P < 0.001$ versus the wild type.

Reduced Ca^{2+} sensitivity in perfused $S100A1^{-/-}$ hearts. β-Adrenergic agonists activate adenyl cyclase and stimulate cAMP-dependent protein kinase (cAPK)-dependent phosphorylation of PLB, resulting in enhanced systolic force generation by indirectly increasing Ca^{2+} release from the SR during cardiac contraction-relaxation cycles (26). Based on Ca^{2+}/S100A1-dependent stimulation of adenylate cyclase (13) and the manifold effects of S100 proteins on protein phosphorylation in vitro (8), defective β-adrenergic signaling could be a possible mechanism involved in the S100A1 null phenotype. We therefore analyzed if S100A1-deficient cardiomyocytes could actually respond to β-adrenergic stimulation. In these experiments, total left-ventricular β-adrenoceptor densities were similar among the three S100A1 genotypes (Fig. 3A). Likewise, immunoblots using a phosphospecific antibody re-

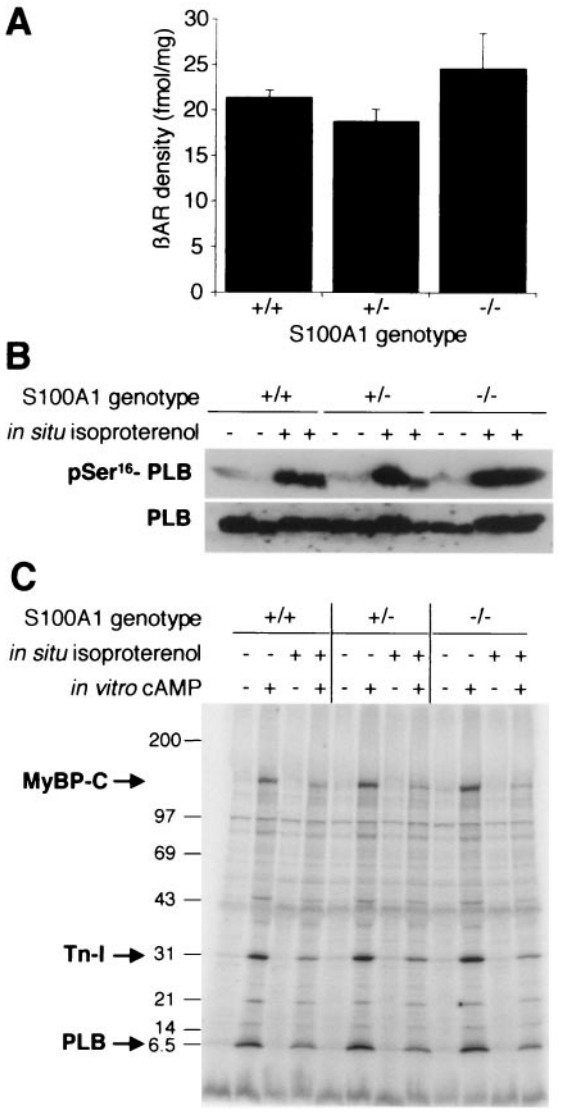

FIG. 3. Normal β-adrenergic pathway in S100A1-deficient mice. (A) β-Adrenoceptor (βAR) densities in left-ventricle membrane protein preparations. (B) Isoproterenol-induced phosphorylation of PLB. Results from two animals per genotype are shown. Hearts were perfused in situ with or without 1 μM isoproterenol, and protein extracts of left ventricles were analyzed with a phospho-Ser^{16}-specific antibody. The lower panel shows a similarly loaded blot analyzed for total PLB as a loading control. (C) Autoradiograph of a representative back-phosphorylation assay. Left-ventricle protein extracts from control (−) or isoproterenol-stimulated (+) hearts were subjected to in vitro phosphorylation assays with or without cAMP addition and separated by SDS–5 to 18% polyacrylamide gel electrophoresis. Positions of mass standards are indicated on the left (in kilodaltons). MyBP-C, myosin-binding protein C; Tn-I, troponin I.

vealed that PLB phosphorylation in intact isoproterenol-perfused hearts was undiminished in S100A1 gene-targeted mice relative to that in wild-type littermates (Fig. 3B). Similar results were obtained in back-phosphorylation assays, where extracts from isoproterenol-perfused and control hearts were subjected to in vitro protein kinase assays. Back-phosphorylation assays provide an indirect readout for physiological phosphorylation states, as residues already phosphorylated in vivo cannot be radiolabeled during the subsequent in vitro kinase reaction (27, 35). The autoradiograph in Fig. 3C shows that pretreatment with isoproterenol blocked the cAMP-dependent in vitro phosphorylation of PLB to the same extent (~65% reduction) in all genotypes. Similar results were also obtained for troponin I (~65% reduction) and myosin-binding protein C (>80% reduction), the other major physiological cardiac cAPK substrates, whose phosphorylation is involved in modulating the sarcomeric Ca^{2+} sensitivity in response to β-adrenergic stimulation (16, 23).

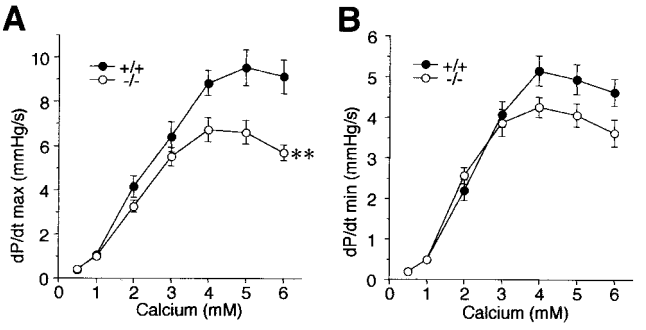

FIG. 4. Inotropic (A) and lusitropic (B) responses in hearts perfused in situ with various Ca^{2+} concentrations. **, $P < 0.001$ versus wild type. $n = 7$ per genotype; values are in thousands.

As these data indicated that β-adrenergic signaling pathways are unaffected in $S100A1^{-/-}$ hearts, we tested if the impaired inotropic and lusitropic responses could be due to a reduced Ca^{2+} sensitivity. For this purpose, mouse hearts were perfused in situ with various Ca^{2+} concentrations (Fig. 4). In these experiments, $S100A1^{-/-}$ hearts again had a significantly reduced inotropic response to increased Ca^{2+} concentrations compared to hearts from wild-type littermates (Fig. 4A). While the lusitropic Ca^{2+} response was also reduced in S100A1 null mice (Fig. 4B), this was statistically not significant ($P = 0.054$). In Ca^{2+} perfusion experiments, potential defects in Ca^{2+} release from the SR are expected to be compensated by increased Ca^{2+} influx via sarcolemmal voltage-dependent Ca^{2+} channels. This experiment therefore indicates that the reduced force generation in S100A1 null mice is at least in part due to a molecular defect in a terminal aspect of excitation-contraction coupling, possibly at the level of the sarcomere.

Reduced basal contractile function following chronic pressure overload in S100A1 null mice. To test if reduced contractile function of $S100A1^{-/-}$ and $S100A1^{+/-}$ hearts leads to an exacerbation of the phenotype in response to chronic hemodynamic stress, TAC were performed surgically to increase left-ventricular afterload (8 to 10 animals per genotype; 5 months of age). In contrast to sham operations, chronic pressure overload by TAC for 3 weeks resulted in a normal adaptive hypertrophy in all mice with increased left ventricle masses (Fig. 5A) and ~10-fold upregulation of left-ventricular atrial natriuretic factor (ANF) mRNA levels as a molecular hypertrophy marker (38) (Fig. 5B). However, despite the normal hypertrophic response, in $S100A1^{-/-}$ mice TAC caused a marked functional depression of basal left-ventricular contractility (dP/dt_{max}) and relaxation (dP/dt_{min}) rates relative to

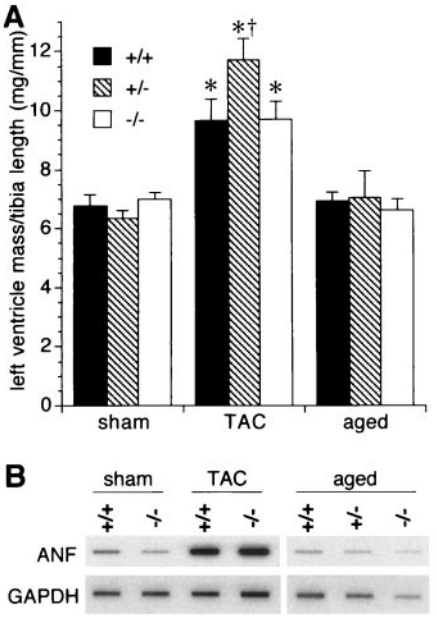

FIG. 5. Left-ventricular hypertrophy indicators. (A) Wet weights of left ventricles normalized by tibia length from 5-month-old (sham and TAC) and 16-month-old (aged) mice. (B) RNA blot analysis of left ventricles using ANF and GAPDH cDNA probes. *, $P < 0.01$ versus the respective sham-operated group; †, $P < 0.05$ versus the −/− TAC-treated group.

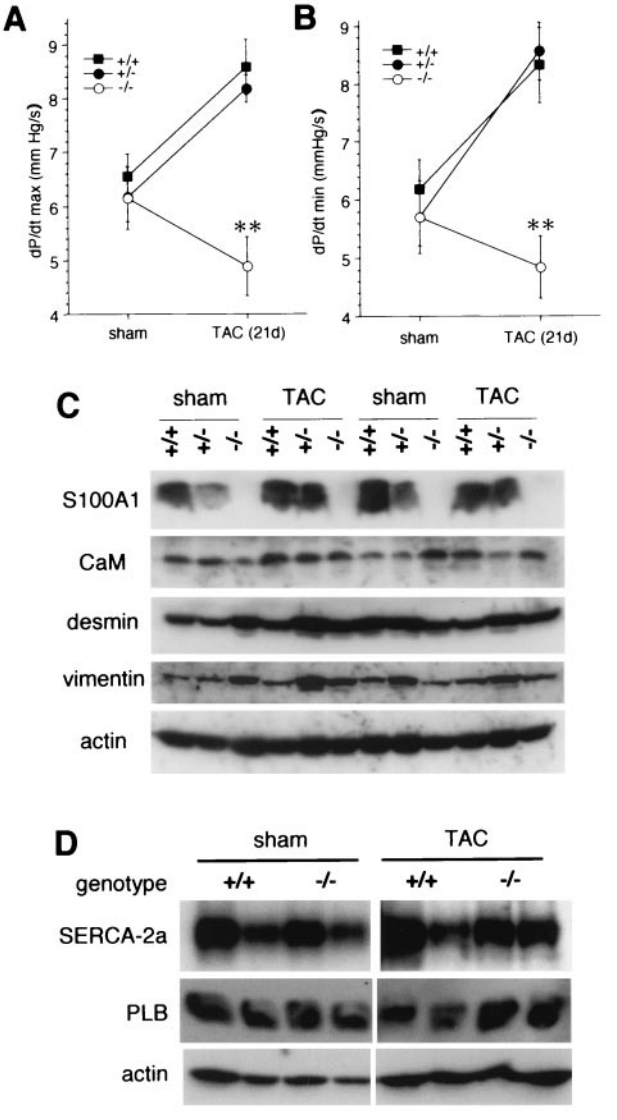

FIG. 6. Functional response to chronic hemodynamic stress induced by 3-week TAC compared to sham-operated littermates. (A and B) Basal left-ventricular contractility (A) and relaxation (B) rates were measured in microcatheterized intact animals. Values are in thousands. (C) Immunoblot analysis of heart extracts of sham-operated and TAC-treated mice, probed with the antibodies indicated on the left. CaM, calmodulin. (D) SERCA-2a and PLB levels in sham- and TAC-treated wild-type and S100A1 null mice. **, $P < 0.001$ versus wild type and heterozygotes.

sham-operated controls (Fig. 6A and B). In contrast, TAC resulted in a compensatory inotropic and lusitropic enhancement of left-ventricular function in wild-type littermates and, surprisingly, in heterozygotes (Fig. 6A and B).

To identify a basis for the apparent S100A1 haploinsufficiency for the acute response to β-adrenergic stimulation (Fig. 2B to D) but not for the adaptive response to chronic pressure overload (Fig. 6A and B), we compared S100A1 protein levels in sham-operated mice and TAC-treated mice. Surprisingly, this analysis revealed that S100A1 protein levels in heterozygotes were upregulated from approximately half of wild-type levels in the control group (three animals per genotype) to levels equal to those in the wild type (in five of six animals) in the TAC-treated group (Fig. 6C). In contrast, levels of calmodulin, another EF hand Ca^{2+}-binding protein, were essentially identical in all animals. Additional immunoblots revealed that there were no systematic differences in desmin (as a cardiomyocyte marker) and vimentin (as a fibroblast marker) levels between the different genotypes in either the sham- or TAC-treated group. This indicates that the contractile dysfunction in $S100A1^{-/-}$ mice is not caused by cardiomyocyte loss or increased fibrosis and was supported by picrosirius red histochemistry of a limited number of left ventricles ($n = 4$ to 6), which revealed similar percentages of interstitial collage in all three genotypes (data not shown). Likewise, there were also no changes in SERCA-2a or PLB levels between the different genotypes in the sham- or TAC-treated groups (Fig. 6D), demonstrating that the contractile deficit in S100A1 null mice is not simply the result of an altered SERCA-2/PLB ratio.

Cardiac function in aged S100A1 gene-targeted mice. Reduced left-ventricular contractile function in other mouse genetic models leads to activation of initially compensatory cardiomyocyte remodeling processes which ultimately become maladaptive and result in chronic hypertrophic or dilated cardiomyopathies and heart failure (1, 4, 7, 28, 39, 42). We therefore investigated if S100A1 deficiency leads to an age-related cardiomyopathy in our mice. While maximal left-ventricular inotropic and lusitropic rates further declined in $S100A1^{-/-}$ and $S100A1^{+/-}$ animals between 5 and 16 months of age, this was less pronounced than the age-related decline in wild-type

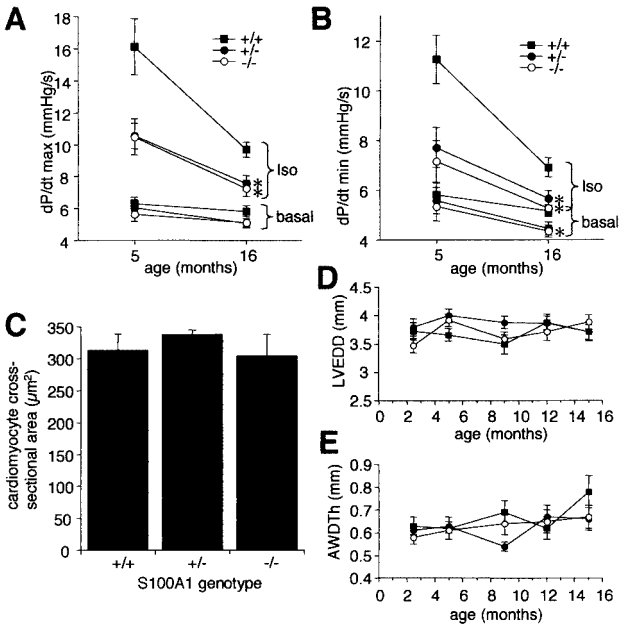

FIG. 7. Cardiac parameters in aged mice. (A and B) Basal and isoproterenol (2 ng)-stimulated inotropic (A) rates and lusitropic (B) rates in 16-month-old versus 5-month-old mice. Values are in thousands. (C) Left-ventricular cardiomyocyte cross-sectional areas in 16-month-old mice. (D) Left-ventricle end diastolic diameters (LVEDD) in groups of 10 mice per genotype from 10 weeks to 16 months of age. (E) Anterior wall diastolic thicknesses (AWDTh) in the same groups of animals shown in panel D. Posterior wall thicknesses were similar to those shown here (data not shown). *, $P < 0.05$ versus wild type.

littermates (Fig. 7A and B). However, left-ventricle and heart weights (Fig. 5A and data not shown), left-ventricular ANF mRNA levels (Fig. 5B), and cardiomyocyte cross-sectional areas (Fig. 7C) were normal in 16-month-old S100A1 mutant mice. Likewise, a long-term echocardiographic study of 10 animals per genotype revealed normal diastolic left-ventricular diameters (Fig. 7D) and wall thicknesses (Fig. 7E) in S100A1 null and heterozygous mice from 10 weeks to 15 months of age. Taken together, these results demonstrate that the reduced contractile function by itself does not lead to a spontaneous hypertrophic or dilated pathology under basal conditions in S100A1 mutant mice.

DISCUSSION

Ca^{2+} ions are essential for cardiomyocyte contractions by binding to the sarcomeric EF hand protein troponin-C, which alleviates its inhibition of actomyosin interactions and allows movement of the myosin-containing thick filaments along actin-containing thin filaments (recently reviewed in references 4, 26, and 42). Cardiac contraction-relaxation cycles are initiated by activation of plasma-membrane voltage-dependent L-type Ca^{2+} channels, which in turn stimulates the massive release of Ca^{2+} from the SR into the cytoplasm by the ryanodine receptors (SR Ca^{2+} release channels). Contractions are terminated and relaxation occurs following the reuptake of Ca^{2+} into the SR via the SR Ca^{2+} pump SERCA-2. β-Adrenergic stimulation leads to enhanced sarcomeric force production by synchronizing Ca^{2+} release by ryanodine receptors (43) and by cAPK-dependent phosphorylation of the SERCA-2 inhibitor PLB (26). This increases relaxation rates by enhancing Ca^{2+} reuptake into the SR and has a positive inotropic effect by increasing the Ca^{2+} pool available for subsequent release cycles. Ca^{2+} also plays a crucial role in regulating cardiomyocyte growth. Tonic increases in diastolic Ca^{2+} levels as a result of chronically increased workloads or biomechanical impairment of contractile function stimulate cardiomyocyte hypertrophy in a pathway dependent on the protein phosphatase calcineurin and the transcription factor NF-AT3/GATA4 (4, 30, 42), which can be genetically attenuated by increasing SR Ca^{2+} reuptake through PLB elimination (29).

The data presented here show that the S100A1 Ca^{2+}-binding protein has important cardiac functions in vivo by regulating the extent of enhanced contractility in response to acute inotropic stimulation (Fig. 2) and the functional adaptation to chronic hemodynamic stress (Fig. 6). Haploinsufficiency for the acute β-adrenergic response (Fig. 2), but normal functional adaptation to chronic pressure overload in heterozygotes that correlates with a compensatory S100A1 upregulation (Fig. 6), indicates that remarkably high S100A1 levels in left-ventricular cardiomyocytes are necessary for normal heart function. Our data are fully consistent with a recent report (31) that adenovirus-mediated overexpression of S100A1 enhances contractility in isolated rabbit cardiomyocytes and engineered rat heart tissue. This supports the notion that the phenotype reported here is the genuine consequence of S100A1 deletion rather than the result of secondary changes, e.g., compensatory upregulation of other members of the S100 gene family. Like many other proteins, S100A1 levels are severely reduced in end-stage cardiac failure (36). Given the results of our study that high S100A1 levels are required for maximal cardiac contractility, it may therefore be speculated that reduced S100A1 levels contribute to the functional deterioration in human cardiomyopathies. To address this issue in the future, it will clearly be important to analyze the impact of S100A1 deletion or overexpression on contractility in established experimental cardiomyopathy models.

In contrast to other mouse mutants with impaired cardiac function, the S100A1 deletion phenotype model is to our knowledge the only genetic model where a cardiac contractile dysfunction (Fig. 2, 4, and 6) does not automatically lead to unprovoked age-dependent cardiomyopathic features under baseline conditions (Fig. 5 and 7). This absence of a degenerative phenotype is most likely explained by the fact that S100A1 null mice have a largely normal hemodynamic function at rest. Taken together, the pairing of normal baseline cardiac function and absence of age-related cardiomyopathies with impaired adaptation to acute and chronic hemodynamic stress in S100A1 null mice therefore demonstrates that the S100A1 protein has a specific function in the cardiac reserve. It is clear that the phenotype described here reflects specific effector functions of S100A1 and not simply Ca^{2+}-buffering functions, as the latter would be expected to result in higher cytoplasmic Ca^{2+} levels in mutant animals with concomitantly increased inotropic responses and an enhanced calcineurin-dependent hypertrophic response.

Numerous in vitro S100A1 targets have previously been

identified that could theoretically be involved in the S100A1 null phenotype. However, the normal cardiac baseline function and histology in S100A1 null mice indicate that cytoskeletal targets such as tubulin polymerization (8) or desmin filament assembly (15) are unlikely to be regulated by S100A1 in vivo. Moreover, although desmin deletions cause decreased force production and slower relaxation, null and point mutations result in cardiomyopathies (6, 28) in contrast to our mice. Likewise, efficient PLB phosphorylation as a downstream target of the β-adrenergic pathway in S100A1 null mice (Fig. 3) rules out Ca^{2+}/S100A1 effects on adenylate cyclase (13) as a major in vivo target. An interesting in vitro target in the context of the S100A1 deficiency phenotype is the skeletal muscle ryanodine receptor (44). Assuming that Ca^{2+}/S100A1 would similarly increase the open probability of the structurally distinct cardiac ryanodine receptor isoform, this could provide an explanation for the inotropic defect, but not the lusitropic defect, in S100A1 null mice. However, the reduced inotropic response of S100A1$^{-/-}$ hearts in Ca^{2+} perfusion experiments (Fig. 4), where increased Ca^{2+} influx through L-type Ca^{2+} channels can compensate for reduced SR Ca^{2+} release, suggests that the S100A1 protein has a more downstream role in excitation-contraction coupling, possibly by modulating the sarcomeric Ca^{2+} sensitivity. The goal of future studies will be to identify the molecular targets that are affected by reduced S100A1 levels and contribute to the phenotype. This may also answer the question of why such high S100A1 levels are required for normal function (such that reduced levels in heterozygotes are insufficient for the acute stress response), which could reflect either low-affinity interactions with its targets or high cellular concentrations of S100A1 effectors.

The upregulation of left-ventricular S100A1 levels in heterozygotes in response to chronic afterload increase (Fig. 6C) is reminiscent of the right ventricular upregulation of S100A1 in normal pigs in response to pulmonary hypertension (12). In contrast to the porcine model, relative left-ventricular S100A1 levels were not upregulated in response to TAC in our wild-type mice (Fig. 6C). This apparent discrepancy can be reconciled by the consideration that S100A1 levels are much lower in the right ventricle than in the left ventricle, possibly reflecting lower physiological workloads, and indicates that left-ventricular S100A1 is preset at the maximal required level for the cardiac reserve in wild-type animals. The S100A1 gene contains several cAMP response elements (25) that could mediate transcriptional upregulation in response to chronic hemodynamic stress as a result of increased β-adrenergic stimulation. However, the mechanism by which this affects left-ventricular S100A1 levels in heterozygotes but not in the wild type remains an enigma. In this context, it will be interesting to determine if chronic β-adrenergic stimulation (by chronic isoproterenol application from implanted minipumps or by crossing the S100A1 deletion with cardiac β-adrenoceptor overexpressing transgenic mice) is sufficient to upregulate S100A1 levels in heterozygotes.

Genetic analyses of protein functions are often hampered by functional redundancy in multigene families. In this regard, the cardiac phenotype in mice lacking the S100A1 gene and haploinsufficiency for the acute β-adrenergic response are remarkable for a representative of a multigene family with 20 members. These data indicate that there is little functional redundancy among S100 proteins in the adult heart. S100A1 is highly expressed in the embryonic heart, suggesting a potential function in cardiac development (25). While our data demonstrate that S100A1 is not essential, it will be interesting to determine if there are compensatory mechanisms involving other S100 genes that substitute for the loss of S100A1 during cardiac development.

ACKNOWLEDGMENTS

We thank members of the WEHI Genetically Modified Mouse Laboratory for help in generating the S100A1-targeted strain, the Baker Institute Biomedical Research Unit for animal care and breeding, Elodie Percy for help with β-adrenoceptor density measurements, Daphne Hards for advice on immunohistochemistry, Dominic Autelitano for cDNAs, and Duncan Campbell, Diane Fatkin, and Robert Graham for comments on the manuscript.

This work was supported by grants from the National Health and Medical Research Council of Australia (NHMRC). X.-J.D., B.E.K., and J.H. are NHMRC Fellows.

REFERENCES

1. **Arber, S., J. J. Hunter, J. Ross, M. Hongo, G. Sansig, J. Borg, J. C. Perriard, K. R. Chien, and P. Caroni.** 1997. MLP-deficient mice exhibit a disruption of cardiac cytoarchitectural organization, dilated cardiomyopathy, and heart failure. Cell **88:**393–403.
2. **Baudier, J., E. Bergeret, N. Bertacchi, H. Weintraub, J. Gagnon, and J. Garin.** 1995. Interactions of myogenic bHLH transcription factors with calcium-binding calmodulin and S100a (aa) proteins. Biochemistry **34:**7834–7846.
3. **Chawengsaksophak, K., R. James, V. E. Hammond, F. Köntgen, and F. Beck.** 1997. Homeosis and intestinal tumours in Cdx2 mutant mice. Nature **386:**84–87.
4. **Chien, K. R.** 2000. Genomic circuits and the integrative biology of cardiac diseases. Nature **407:**227–232.
5. **Clapham, D. E.** 1995. Calcium signalling. Cell **80:**259–268.
6. **Dalakas, M. C., K. Y. Park, C. Semino-Mora, H. S. Lee, K. Sivakumar, and L. G. Goldfarb.** 2000. Desmin myopathy, a skeletal myopathy with cardiomyopathy caused by mutations in the desmin gene. N. Engl. J. Med. **342:**770–780.
7. **Dash, R., V. J. Kadambi, A. G. Schmidt, N. Tepe, D. Biniakiewicz, M. J. Gerst, A. M. Canning, W. T. Abraham, B. D. Hoit, S. B. Liggett, J. B. Lorenz, G. W. Dorn II, and E. G. Kranias.** 2001. Interactions between phospholamban and β-adrenergic drive may lead to cardiomyopathy and early mortality. Circulation **103:**889–896.
8. **Donato, R.** 1999. Functional roles of S100 proteins, calcium-binding proteins of the EF-hand type. Biochem. Biophys. Acta **1450:**191–231.
9. **Du, X. J., D. J. Autelitano, R. J. Dilley, B. Wang, A. M. Dart, and E. A. Woodcock.** 2000. β_2-Adrenergic receptor overexpression exacerbates development of heart failure after aortic stenosis. Circulation **101:**71–77.
10. **Du, X. J., X. M. Gao, B. Wang, G. L. Jennings, E. A. Woodcock, and A. M. Dart.** 2000. Age-dependent cardiomyopathy and heart failure phenotype in mice overexpressing β_2-adrenergic receptors in the heart. Cardiovasc. Res. **48:**448–454.
11. **Du, X. J., E. Vincan, D. M. Woodcock, C. A. Milano, A. M. Dart, and E. A. Woodcock.** 1996. Response to cardiac sympathetic activation in transgenic mice overexpressing β_2-adrenergic receptor. Am. J. Physiol. **40:**H630-H636.
12. **Ehlermann, P., A. Remppis, O. Guddat, J. Weimann, P. A. Schnabel, J. Motsch, C. W. Heizmann, and H. A. Katus.** 2000. Right ventricular upregulation of the Ca^{2+} binding protein S100A1 in chronic pulmonary hypertension. Biochem. Biophys. Acta **1500:**249–255.
13. **Fano, G., P. Angelella, D. Mariggio, M. C. Aisa, I. Giambanco, and R. Donato.** 1989. $S100a_0$ protein stimulates the basal (Mg^{2+}-activated) adenylate cyclase activity associated with skeletal muscle membranes. FEBS Lett. **248:**9–12.
14. **Fano, G., V. Marsili, P. Angelella, M. C. Aisa, I. Giambanco, and R. Donato.** 1989. S-$100a_0$ protein stimulates Ca^{2+}-induced Ca^{2+} release from isolated sarcoplasmic reticulum vesicles. FEBS Lett. **255:**381–384.
15. **Garbuglia, M., M. Verzini, I. Giambanco, A. Spreca, and R. Donato.** 1996. Effects of calcium-binding proteins (S-100a(o), S-100a, S-100b) on desmin assembly in vitro. FASEB J. **10:**317–324.
16. **Grün, M., H. Prinz, and M. Gautel.** 1999. cAPK-phosphorylation controls the interaction of the regulatory domain of cardiac myosin binding protein C with myosin-S2 in an on-off fashion. FEBS Lett. **453:**254–259.
17. **Heierhorst, J., B. Kobe, S. C. Feil, M. W. Parker, G. M. Benian, K. R. Weiss, and B. E. Kemp.** 1996. Ca^{2+}/S100 regulation of giant protein kinases. Nature **380:**636–639.

18. **Heierhorst, J., R. J. Mann, and B. E. Kemp.** 1997. Interaction of the recombinant S100A1 protein with twitchin kinase, and comparison with other Ca^{2+}-binding proteins. Eur. J. Biochem. **249:**127–133.
19. **Heierhorst, J., K. I. Mitchelhill, R. J. Mann, T. Tiganis, A. J. Czernik, P. Greengard, and B. E. Kemp.** 1999. Synapsins as major neuronal Ca^{2+}/S100A1-interacting proteins. Biochem. J. **344:**577–583.
20. **Hofmann, M. A., S. Drury, C. Fu, W. Qu, A. Taguchi, Y. Lu, C. Avila, N. Kambham, A. Bierhaus, P. Nawroth, M. F. Neurath, T. Slattery, D. Beach, J. McClary, M. Nagashima, J. Morser, D. Stern, and A. M. Schmidt.** 1999. RAGE mediates a novel proinflammatory axis: a central cell surface receptor for S100/calgranulin polypeptides. Cell **97:**889–901.
21. **Inamoto, S., S. Murao, M. Yokoyama, S. Kitazawa, and S. Maeda.** 2000. Isoproterenol-induced myocardial injury resulting in altered S100A4 and S100A11 protein expression in the rat. Pathol. Int. **50:**480–485.
22. **Kato, K., S. Kimura, H. Haimoto, and F. Suzuki.** 1986. $S100a_0$(aa) protein: distribution in muscle tissues of various animals and purification from human pectoral muscle. J. Neurochem. **46:**1555–1560.
23. **Kentish, J. C., D. T. McCloskey, J. Layland, S. Palmer, J. M. Leiden, A. F. Martin, and R. J. Solaro.** 2001. Phosphorylation of troponin I by protein kinase A accelerates relaxation and crossbridge cycle kinetics in mouse ventricular muscle. Circ. Res. **88:**1059–1065.
24. **Kiewitz, R., C. Acklin, E. Minder, P. R. Huber, B. W. Schafer, and C. W. Heizmann.** 2000. S100A1, a new marker for acute myocardial ischemia. Biochem. Biophys. Res. Commun. **274:**865–871.
25. **Kiewitz, R., G. E. Lyons, B. W. Schäfer, and C. W. Heizmann.** 2000. Transcriptional regulation of S100A1 and expression during mouse heart development. Biochem. Biophys. Acta **1498:**207–219.
26. **Kiriazis, H., and E. G. Kranias.** 2000. Genetically engineered models with alterations in cardiac membrane calcium-handling proteins. Annu. Rev. Physiol. **62:**321–351.
27. **Marx, S. O., S. Reiken, Y. Hisamatsu, T. Jayaraman, D. Burkhoff, N. Rosemblit, and A. R. Marks.** 2000. PKA phosphorylation dissociates FKBP12.6 from the calcium release channel (ryanodine receptor): defective regulation in failing hearts. Cell **101:**365–376.
28. **Milner, D. J., G. E. Taffet, X. Wang, T. Pham, T. Tamura, C. Hartley, A. M. Gerdes, and Y. Capetanaki.** 1999. The absence of desmin leads to cardiomyocyte hypertrophy and cardiac dilation with compromised systolic function. J. Mol. Cell. Cardiol. **31:**2063–2076.
29. **Minamisawa, S., M. Hoshijima, G. Chu, C. A. Ward, K. Frank, Y. Gu, M. E. Martone, Y. Wang, J. Ross, Jr., E. G. Kranias, W. R. Giles, and K. R. Chien.** 1999. Chronic phospholamban-sarcoplasmic reticulum calcium ATPase interaction is the critical calcium cycling defect in dilated cardiomyopathy. Cell **99:**313–322.
30. **Molkentin, J. D., J. Lu, C. L. Antos, B. Markham, J. Richardson, J. Robbins, S. Grant, and E. N. Olson.** 1998. A calcineurin-dependent transcriptional pathway for cardiac hypertrophy. Cell **93:**213–228.
31. **Most, P., J. Bernotat, P. Ehlermann, S. T. Pleger, M. Reppel, M. Börries, F. Niroomand, B. Pieske, P. M. Janssen, T. Eschenhagen, P. Karczewski, G. L. Smith, W. J. Koch, H. A. Katus, and A. Remppis.** 2001. S100A1: a novel regulator of cardiac contractility. Proc. Natl. Acad. Sci. USA **98:**13889–13894.
32. **Nakatani, K., Y. Kawanabe, A. Kato, and T. Tanaka.** 1996. Interaction of propranolol with S100 proteins of the cardiac muscle. Eur. J. Pharmacol. **315:**335–338.
33. **Olson, E. N., H. H. Arnold, P. W. Rigby, and B. J. Wold.** 1996. Know your neighbors: three phenotypes in null mutants of the myogenic bHLH gene MRF4. Cell **85:**1–4.
34. **Passey, R. J., E. Williams, A. M. Lichanska, C. Wells, S. Hu, C. L. Geczy, M. L. Little, and D. L. Hume.** 1999. A null mutation in the inflammation-associated S100 protein S100A8 causes early resorption of the mouse embryo. J. Immunol. **163:**2209–2216.
35. **Probst, W. C., E. C. Cropper, J. Heierhorst, S. L. Hooper, H. Jaffe, F. Vilim, S. Beushausen, I. Kupfermann, and K. R. Weiss.** 1994. cAMP-dependent phosphorylation of *Aplysia* twitchin may mediate modulation of muscle contractions by neuropeptide cotransmitters. Proc. Natl. Acad. Sci. USA **91:**8487–8491.
36. **Remppis, A., T. Greten, B. W. Schäfer, P. Hunziker, P. Erne, H. A. Katus, and C. W. Heizmann.** 1996. Altered expression of the Ca^{2+}-binding protein S100A1 in human cardiomyopathy. Biochim. Biophys. Acta **1313:**253–257.
37. **Ridinger, K., E. C. Ilg, F. X. Niggli, C. W. Heizmann, and B. W. Schäfer.** 1998. Clustered organization of S100 genes in human and mouse. Biochim. Biophys. Acta **1448:**254–263.
38. **Rockman, H. A., R. S. Ross, A. N. Harris, K. U. Knowlton, M. E. Steinhelper, L. J. Field, J. J. Ross, and K. R. Chien.** 1991. Segregation of atrial-specific and inducible expression of an atrial natriuretic factor transgene in an in vivo murine model of cardiac hypertrophy. Proc. Natl. Acad. Sci. USA **88:**8277–8281.
39. **Sato, Y., D. G. Ferguson, H. Sako, G. W. Dorn, V. J. Kadambi, A. Yatani, B. D. Hoit, R. A. Walsh, and E. G. Kranias.** 1998. Cardiac-specific overexpression of mouse cardiac calsequestrin is associated with depressed cardiovascular function and hypertrophy in transgenic mice. J. Biol. Chem. **273:**28470–28477.
40. **Schäfer, B. W., and C. W. Heizmann.** 1996. The S100 family of EF-hand calcium-binding proteins: functions and pathology. Trends Biochem. Sci. **21:**134–140.
41. **Schwenk, F., U. Baron, and K. Rajewsky.** 1995. A cre-transgenic mouse strain for the ubiquitous deletion of loxP-flanked gene segments including deletion in germ cells. Nucleic Acids Res. **23:**5080–5081.
42. **Seidman, J. G., and C. Seidman.** 2001. The genetic basis for cardiomyopathy: from mutation identification to mechanistic paradigms. Cell **104:**557–567.
43. **Song, L.-S., S.-Q. Wang, R.-P. Xiao, H. Spurgeon, E. G. Lakatta, and H. Cheng.** 2001. β-Adrenergic stimulation synchronizes intracellular Ca^{2+} release during excitation-contraction coupling in cardiac myocytes. Circ. Res. **88:**794–801.
44. **Treves, S., E. Scutari, M. Robert, S. Groh, M. Ottolia, G. Prestipino, M. Ronjat, and F. Zorzato.** 1997. Interaction of S100A1 with the Ca^{2+} release channel (ryanodine receptor) of skeletal muscle. Biochemistry **36:**11496–11503.
45. **Tsoporis, J. N., A. Marks, H. J. Kahn, J. W. Butany, P. P. Liu, D. O'Hanlon, and T. G. Parker.** 1998. Inhibition of norepinephrine-induced cardiac hypertrophy in S100β transgenic mice. J. Clin. Investig. **102:**1609–1616.
46. **Xiong, Z., D. O'Hanlon, L. E. Becker, J. Roder, J. F. MacDonald, and A. Marks.** 2000. Enhanced calcium transients in glial cells in neonatal cerebellar cultures derived from S100B null mice. Exp. Cell Res. **257:**281–289.
47. **Zimmer, D. B., E. H. Cornwall, A. Landar, and W. Song.** 1995. The S100 protein family: history, function, and expression. Brain Res. Bull. **37:**417–429.